

Modeling the Sensory Computations of the Olfactory Bulb

Zhaoping Li,

The Rockefeller University, 1230 York Avenue, New York, NY 10021, USA

This is published in *Models of Neural Networks* Vol. 2. Eds. E. Domany, J. L. van Hemmen, and K. Schulten, page 221-251 Springer-Verlag New York, 1995.

1 Introduction

The olfactory system is a phylogenetically primitive part of the cerebral cortex [1]. In lower vertebrates, the olfactory system is the largest part of the telencephalon. It also has a intrinsically simple cortical structure, which in modified form is used in other parts of the brain [1]. The odor molecules of the distal objects to be detected are bound to and crudely recognized by receptor proteins, giving a relatively well defined input signals, compared to the photoreceptor and hair cell activities in vision and audition, for object identities. Hence the olfactory system conceivably handles a relatively simpler computational problem. Having phylogenetic importance and computational simplicity, the olfactory system promises to yield insight on the principles of sensory information processing.

What is the olfactory system trying to compute from its sensory input? It should try to perform some or all of the following tasks: 1. odor detection; 2. if there is only one odor present, odor identification and concentration estimation [3]; 3. if there are multiple odors present, odor segmentation — before identification and concentration estimation can be performed [2][4]; 4. localization of the odor sources [2]. Tasks 1 and 2 should be performed by any olfactory system. Task 3 is often necessary for odor recognition and localization since the olfactory environment is frequently composed of odor mixtures, and any olfactory model should address it. Task 4 is especially important and necessary for animals, such as insects and nocturnal animals, who depend largely on chemical senses in their environment [5][6][2].

The olfactory bulb, the first processing stage after the sensory receptors, is likely to compute towards the computational goals above. It transforms the input signals, represented by the spatiotemporal activation patterns in the receptor cells, to input dependent ((7)[8][9][10]) spatio-temporal oscillatory activities at the output, which are

then sent directly to the olfactory cortex for mammals (Fig 1.)[1]. Hence the bulbar output carries the relevant information about the input odors. The models described in this paper assume that some of the computational goals above are first attempted by the processings in the bulb. The computation in the olfactory cortex cannot be understood without knowing the bulbar processing and outputs.

This article demonstrates the olfactory modelling approach by comprehensive description of two models of the olfactory bulb. One of them [3][4] suggests that the mammalian bulb detects and identifies an odor and its concentration by the amplitudes and phases of the oscillation across the bulb (tasks 1 and 2). Furthermore, it hypothesizes that the bulb detects and identifies a more recent odor input in the presence of another odor — odor segmentation (task 3) — by olfactory adaptation. It suggests that the adaptation should be viewed as a computational strategy instead of as olfactory fatigue. The odor localization task (task 4), however, is not addressed by this model. The other model[2] has a different perspective and emphasizes odor segmentation and localization (tasks 3 and 4), even when the odor objects are not familiar and many odors are simultaneously present. It hypothesizes that the bulb segments or identifies the individual odors by analyzing the correlations in the input temporal fluctuations. As a result, identities and fluctuations of individual odor components are identified from the input mixture. Each component fluctuation, which contains the information about the odor source location, can then be used by higher brain centers to localize the source. The problem is solved by dynamic changes of the synaptic strengths, which are proposed to encode the odor identity.

This article is thus not intended as a complete review of all the modelling and other relevant works in the field, which can be found in the literature [11]. Among other works are studies of odor transduction by receptors [12], detailed computer simulation using biological parameters to reproduce physiological observations [13][14], a model to study macroglomerulus neural response variations to behaviorally relevant input changes in insects [15], a model of efficient coding in the bulb [16], computational studies of olfactory cortex as a content-addressable memory and learning [17][18][19], and a discussion on non-linear neural dynamical processing of odor information [20].

In the next section, some background is given on the olfactory bulb and its sensory receptor inputs. Section 3 presents a model of the neural activities observed in the mammalian bulb. Section 4 shows how this model codes and segments odors. Section 5 presents Hopfield's model [2] of odor identity and fluctuation segmentation in odor mixtures. In section 6, we discuss the differences between these models, their relationships to the computational tasks and environments, and relate the computational approaches used in olfaction to those used in other sensory systems.

2 Anatomical and Physiological Background

The olfactory bulb contains sharply differentiated cell types located on different parallel lamina [1]. Each receptor sends a single unbranched axon to the topmost layer, terminating in one of the spherical regions of neuropil termed glomeruli (Fig. [1] A, B). The receptor axons ramify inside the glomeruli, synapsing on the excitatory mitral cells and the inhibitory short axon cells.

With increased odor concentration, the receptor cell firing rate in vertebrates [21] increases from the spontaneous background of 1 – 3 impulses/second, and may reach 10 – 60 impulses/sec. With an odor pulse delivered to the mucosa, the receptor firing rate increases approximately linearly in time as long as the pulse is not too long, and then terminates quickly, after the odor pulse terminates [21]. More than 100 genes for odor receptors have been identified in mammals [22]. It is not known whether a single type or a few types are expressed in each receptor cell. Most receptor neurons in vertebrates respond in different degrees to a broad range of odor molecules, each response spectrum is unique [12]. Hence there is no clear specificity between odorants and receptor cells, except between pheromone molecules and a subgroup of specialist receptor neurons in insects [12]. There are also inputs from higher olfactory centers to the bulb, but little is known about them [1].

The bulbar cell organization is reviewed in detail by Shepherd [1]. The main cell types of the mammalian bulb are the excitatory mitral cells and the inhibitory granule cells at different cell layers (Fig. 1B). Each mitral cell receives inputs from one or several glomeruli [12]. The granule cells inhibit, and receive excitatory inputs from, the local mitral cells by local dendrodendritic synapses [1] activated by graded presynaptic depolarization. They also receive additional inputs from the mitral cell axon collaterals. The outputs of the bulb are carried by the mitral cell axons; while central feedbacks to the bulb are directed to the granule cells [1].

The activities in the glomeruli layer is odor dependent [9][23]. Stimulation with odors causes an onset of high-amplitude bulbar oscillations, which may be detected by surface EEG electrodes and which returns to low-amplitude oscillations upon the cessation of odor stimulus [7]. Since the odor stimulation is usually synchronized with respiration, the EEG [7][24] shows a high amplitude oscillation arising during the inhalation and stopping early in the exhalation (Fig.2 B). However, respiration itself does not seem to have an effect on bulbar activities [25]. The oscillation is an intrinsic property of the bulb itself, persisting after central connections to the bulb are cut off [20][26]. However, Freeman and coworkers also reported that the central inputs [27] influence oscillation onset, which exists only in motivated animals. Nevertheless, oscillation disappears when the nasal air flow is blocked [24], although the same group reported that it can be present without odor inputs [7]. In invertebrates, the oscillation activities exist without odor inputs, but are modulated by odors [28]. The oscillation bursts have a peak frequency in the range of 35-90 Hz in mammals [24].

Different parts of the bulb have the same dominant frequency but different amplitudes and phases [24][8]. A specific odor input, subject to behavioral conditioning, sets a specific oscillation pattern [8][10].

There are roughly 1000 receptor axons and dendrites from 25 mitral cells in each glomerulus, while there are about 200 granule cells for each mitral cell [1]. A rabbit has about 50,000 mitral cells [1]. Both the mitral and granule cells have a non-linear input-output relationship (Fig. 1C, [27]), and a membrane time constant of 5 – 10 milliseconds [29]. Very little is known about the strength of the synapses in the olfactory bulb.

3 Modeling the neural oscillations in the olfactory bulb

The fact that the oscillatory patterns in the bulb correlate with odor inputs and disappear when air flow is blocked indicates that the odor information is very likely carried in the neural oscillation activities. Before discussing how such activities code odors, we present a model to reproduce the physiologically observed oscillations. The computational issue of odor coding and segmentation will then become apparent by analyzing the dependence of oscillatory activities on the receptor and centrifugal inputs, as will be explained in the next section.

3.1 General model structure

This model [3] attempts to include enough physiological realism to contain the essential computational components and facilitate experimental comparison, yet, nevertheless retains sufficient simplicity to avoid superfluous details. Both M , the number of granule cells, and N , the number of mitral cells, as well as their ratio M/N are much reduced from reality in the simulations, although the mathematical analysis imposes no limit on their actual values. Excitation and inhibition are kept in balance by correspondingly increasing the strength of the granule cell (inhibitory) synapses.

Determining how to wire each receptor to the correct glomerulus and then to the mitral cells for optimal olfactory computation [12][16], is a major computational problem. However, this requires better experimental knowledge of receptor response spectrum to odors than is currently available. Our model thus ignores the glomeruli structure and regards receptor cells as effectively giving inputs I_i onto the i^{th} mitral cell for $1 \leq i \leq N$. This input vector I is a superposition of a true odor signal I_{odor} and a background input $I_{background}$, i.e. $I = I_{odor} + I_{background}$. I_{odor} is determined by odor pattern $P_{odor,i}$ for $1 \leq i \leq N$. We use the approximation, based on experimental findings [30], that for low odor intensity, the direction of vector P_{odor} depends

only on the input odor identity, while its length or amplitude increases with the odor concentration.

Similarly, the central inputs to the granule cells are modelled as a vector $I_c = I_{c,background} + I_{c,control}$, where $I_{c,background}$ is the background signal to the granule cells. $I_{c,control}$ is the active central input that serves some computational purpose as will be discussed in the next section. For the moment, it is assumed that $I_{c,control} = 0$.

Each $I_{odor,i}$ is taken to be excitatory. We model the I_{odor} to increase in time during inhalation, as observed in experiment [21]. Because of the odor absorption by the lungs, as odors are necessarily highly soluble in water [31], I_{odor} is modelled to exponentially return toward the ambient during exhalation, see Fig. 2A. Both $I_{background}$ and $I_{c,background}$ do not change during a sniff cycle, their scales being such that when $I_{odor} = 0$, most of the mitral and granule cells have their cell internal states just below maximum slope points on their input-output functional curves.

Each cell is modelled as one unit [3] under the assumption of short dendritic electrotonic lengths [1]. The state variables, modelling the membrane potentials, are respectively $X = \{x_1, x_2, \dots, x_N\}$ and $Y = \{y_1, y_2, \dots, y_M\}$ for mitral and granule cells. Their outputs are respectively, $G_x(X) = \{g_x(x_1), g_x(x_2), \dots, g_x(x_N)\}$ and $G_y(Y) = \{g_y(y_1), g_y(y_2), \dots, g_y(y_M)\}$. Both g_x and g_y model the probability of the cell firing or firing rate, their functional forms resemble their physiological correlate (Fig. 1C). They have a gain or slope that is approximately zero before the state when the cell response deviates from zero, modelling the firing threshold. This gain becomes large immediately after the threshold. Such non-linearity is essential for the proposed odor computations.

The dynamic equations for the cell population is modelled as

$$\begin{aligned} dX/dt &= -H_o G_y(Y) - \alpha X + I, \\ dY/dt &= W_o G_x(X) - \alpha Y + I_c. \end{aligned} \tag{1}$$

where $\alpha = 1/\tau$, and $\tau = 7$ milliseconds is the cell time constant, assumed to be the same for both cell populations for simplicity. Weak random noise with a correlation time of roughly 10 milliseconds is added to I and I_c to simulate the fluctuations in cell potentials. The matrices H_o and W_o have non-negative elements and model the synaptic connections. Hence $(H_o)_{ij} g_y(y_j)$ models the inhibition from the j^{th} granule to the i^{th} mitral cell, and $(W_o)_{ji} g_x(x_i)$ is the reciprocal excitation. The cell indices i and j approximate cell locations in the bulb (assuming periodic boundary conditions: the N^{th} mitral and the M^{th} granule cells are next to the first mitral and granule cells respectively). Local interaction implies that $(H_o)_{ij}$ and $(W_o)_{ji}$ are non-zero only when $i \approx (N/M)j$, i.e., H_o and W_o are near-diagonal matrices for $N = M$.

3.2 The olfactory bulb as a group of coupled non-linear oscillators

Computer simulations demonstrate that our model captures the major known effects of the real bulb. In the example of 10 mitral and 10 granule cells, the model bulb exhibits the following. (1), Neural oscillations rise with inhalations and fall with exhalations; (2), all cells oscillate coherently with the same frequency which may depend on inputs; and (3), different odor inputs induce different amplitude and phase patterns in cells, and some, including the zero-odor input, do not induce any coherent oscillations. All of the above agree qualitatively with what are observed in physiology, as demonstrated in Fig. 2 ([7][24]). Furthermore, observation (3) demonstrates the model's capabilities as a pattern classifier.

Such agreement between the model and real bulbs can be understood using the following analysis. First, concentrating on the oscillations, notice that a system such as:

$$\begin{aligned} dx/dt &= -\omega y - \alpha x \\ dy/dt &= \omega x - \alpha y \end{aligned} \quad \text{or} \quad d^2x/dt^2 + 2\alpha dx/dt + (\omega^2 + \alpha^2)x = 0 \quad (2)$$

describes a damped oscillator of frequency ω oscillating with time t as

$$x(t) = r_o e^{-\alpha t} \sin(\omega t + \phi)$$

where α is the dissipation constant and r_o , ϕ the initial amplitude and phase. When $\alpha = 0$, the oscillator trajectory in the x-y space is a circle with radius r_o . This system resembles a coupled pair of mitral and granule cells, with external inputs $i(t)$ and $i_c(t)$ respectively,

$$\begin{aligned} dx/dt &= -h \cdot g_y(y) - \alpha x + i(t), \\ dy/dt &= w \cdot g_x(x) - \alpha y + i_c(t). \end{aligned} \quad (3)$$

This is the scalar version of equation (1), with each upper case letter which represented a vector or matrix replaced by a lower case one representing a scalar. The differences between (2) and (3) are mostly the non-linearity of g_x and g_y and the existence of the external inputs. Stationary external inputs can be eliminated by a shift of origin in x-y space. Let the equilibrium point of this system be (x_o, y_o) such that

$$\begin{aligned} dx_o/dt &= -h \cdot g_y(y_o) - \alpha x_o + i = 0, \\ dy_o/dt &= w \cdot g_x(x_o) - \alpha y_o + i_c = 0. \end{aligned} \quad (4)$$

Define $x' \equiv x - x_o$, $y' \equiv y - y_o$, then

$$\begin{aligned} dx'/dt &= -h(g_y(y) - g_y(y_o)) - \alpha x', \\ dy'/dt &= w(g_x(x) - g_x(x_o)) - \alpha y'. \end{aligned}$$

If $g_y(y) - g_y(y_o) \propto y'$ and $g_x(x) - g_x(x_o) \propto x'$, a direct comparison with equation (2) can be made. h and w are accordingly related to the oscillation frequency and α to

the damping constant. Indeed, when $\alpha = 0$, x and y oscillate around (x_o, y_o) in a closed curve

$$R \equiv \int_{x_o}^{x_o+x'} w(g_x(s) - g_x(x_o))ds + \int_{y_o}^{y_o+y'} h(g_y(s) - g_y(y_o))ds = \text{constant} \geq 0$$

which is a circle if $wg_x = hg_y$ are identical linear functions. With non-zero α and monotonic g_x and g_y , the trajectory spirals toward (x_o, y_o) as R decreases to zero:

$$dR/dt = -\alpha w(g_x(x) - g_x(x_o))(x - x_o) - \alpha h(g_y(y) - g_y(y_o))(y - y_o) \leq 0$$

i.e., the oscillation is damped. So we see that a pair of coupled mitral and granule cells can be approximated as a non-linear damped oscillator.

For small amplitudes, the frequency can be calculated by a linear approximation around the (x_o, y_o) :

$$\begin{aligned} dx/dt &= -h \cdot g'_y(y_o)y - \alpha x \\ dy/dt &= w \cdot g'_x(x_o)x - \alpha y \end{aligned} \quad (5)$$

where (x, y) is now the deviation from (x_o, y_o) . The solution is $x(t) = r_o e^{-\alpha t} \sin(\omega t + \phi)$ with frequency $\omega = \sqrt{hwg'_x(x_o)g'_y(y_o)}$.

Under realistic conditions, the odor inputs change on the time scale of the breathing cycle (the same is true when central inputs are concerned, see below). However, since this change is much slower than the oscillation period ≈ 25 milliseconds, the external inputs can be seen as only adiabatically changing. In other words, the input dependent oscillation origin (x_o, y_o) shifts slowly with i and i_c . The oscillation frequency ω shifts accordingly by its dependence on (x_o, y_o) . The frequency of this neural oscillator can thus be designed by the synaptic connections h and w and fine-tuned by the external inputs. This is how the scales of H_o and W_o are chosen to have the model oscillate in the physiologically observed frequency range.

Imagine a group of N such oscillators coupled together by synaptic interactions between cells in different oscillators; it is then a group of coupled non-linear oscillators. This is exactly the case in the olfactory bulb. That there are many more granule cells than mitral cells only means that there is more than one granule cell in each oscillator. For small amplitude oscillations [27], this group can be mathematically approximated as linear oscillators. Proceeding analogously as from (3) to (5), we can start from equation (1) to the analog of (5)

$$\begin{aligned} dX/dt &= -H_o G'_y(Y_o)Y - \alpha X \equiv -HY - \alpha X, \\ dY/dt &= W_o G'_x(X_o)X - \alpha Y \equiv WX - \alpha Y. \end{aligned} \quad (6)$$

where $G'_x(X_o)$ and $G'_y(Y_o)$ are diagonal matrices with elements: $[G'_x(X_o)]_{ii} = g'_x(x_{i,o})$, $[G'_y(Y_o)]_{jj} = g'_y(y_{j,o})$. Since only the mitral cells send bulbar outputs, we concentrate on them by eliminating Y :

$$\ddot{X} + 2\alpha\dot{X} + (A + \alpha^2)X = 0 \quad (7)$$

where $A \equiv HW = H_o G'_y(Y_o) W_o G'_x(X_o)$. This is the equation for a system of N coupled oscillators (cf. equation (2)). The i^{th} oscillator follows the equation

$$\ddot{x}_i + 2\alpha\dot{x}_i + (A_{ii} + \alpha^2)x_i + \sum_{j \neq i} A_{ij}x_j = 0 \quad (8)$$

The first three terms are for a single (i^{th}) oscillator (cf. equation (2)). $A_{ij} = \sum_l (H_o)_{il} g'_y(y_{l,o}) (W_o)_{lj} g'_x(x_{j,o}) \geq 0$ is the coupling strength from the j^{th} to the i^{th} oscillator. It originates from the j^{th} to the i^{th} mitral cell via the intermediate granule cells in the connection path. Thus, local synaptic connections imply local oscillator connections, or in other words, A is near-diagonal. However, unlike a single oscillator, the group is no longer damped and can spontaneously oscillate, induced by the coupling A , as we will see next.

3.3 Explanation of bulbar activities

Let us see how this model can explain the bulbar activities. First, the single oscillator analysis (eqs. (2)(5)) predicts that local mitral cells oscillate with a 90° phase lead over the local granule cells. This is observed in physiological experiments [32].

Second, the model predicts that the oscillation should have the same dominant frequency everywhere in the bulb. One can see this by noticing that equation (7) has N independent mode solutions. The k^{th} mode is

$$X \propto X_k e^{-\alpha t \pm i\sqrt{\lambda_k} t} \quad (9)$$

where X_k and λ_k for $k = 1, 2, \dots, N$ are eigenvectors and eigenvalues of A . (Fig. [3] gives examples of oscillation modes in a coupled oscillator system.) Each mode has frequency $Re\sqrt{\lambda_k}$, where Re means the real part of a complex number.

$$Re(-\alpha \pm i\sqrt{\lambda_k}) > 0 \quad (10)$$

for some k , as can happen for complex λ_k , the amplitude of the k^{th} mode will increase with time. Starting from an initial condition of arbitrarily small amplitudes, the mode satisfying (10) with the fastest growing amplitude will dominate the output, the non-linear effect will suppress the other modes, and the final output will be a single “mode” in a non-linear regime. In that case, although each oscillator has its own amplitude and phase described by the components of X_k , they all share the same oscillation frequency $Re\sqrt{\lambda_k}$, as observed in the experiments [24][8].

The third consequence is that the oscillation phase will have a non-zero gradient across the bulb. Each oscillator oscillates only when the neighboring oscillators give a driving force $F_i = -A_{ij}x_j$ which overcomes the damping force $-2\alpha\dot{x}_i$ (cf. Eq. (8)). This means the neighbor oscillation x_j should have a component that is parallel to $-\dot{x}_i$ or has a phase difference from x_i , generating a non-zero phase gradient field

across the bulb, as observed physiologically [7][24]. This is not necessarily true if mitral-to-mitral or other couplings exist to change the oscillator coupling nature [3], however, there is still not much evidence for mitral-to-mitral connections [1].

The fourth consequence is the experimentally observed rise and fall of oscillations with inhalation and exhalation. This is because growing oscillations require large enough λ_k to satisfy $Re(-\alpha \pm i\sqrt{\lambda_k}) > 0$ for some k . This in turn implies large matrix elements of $A = H_o G'_y(Y_o) W_o G'_x(X_o)$, i.e., large gains G' 's. Thus (X_o, Y_o) should be near the high slope (gain) region of g_x and g_y functions past the threshold. As in the single oscillator case, (X_o, Y_o) depends on the odor input. When the central inputs are constant,

$$\begin{aligned} dX_o &\approx (\alpha^2 + HW)^{-1} \alpha dI \\ dY_o &\approx (\alpha^2 + WH)^{-1} W dI \end{aligned} \tag{11}$$

Before inhalation, (X_o, Y_o) is in the low gain region below the threshold so that none of the modes satisfies (10), and the equilibrium point (X_o, Y_o) is thus stable. Inhalation, $dI > 0$, pushes (X_o, Y_o) into the higher gain region, making inequality (10) possible for some k . (X_o, Y_o) then becomes unstable and the k^{th} mode emerges from noise to visible oscillations across the bulb. Exhalation reverses this situation and the oscillations cease.

4 A model of odor recognition and segmentation in the olfactory bulb

Having successfully modelled the bulbar oscillation phenomena, we now discuss the cognitive value of this model for olfactory computation.

4.1 Emergence of oscillations detects odors; patterns of oscillations code the odor identity and strength.

Odor inputs I_{odor} influence the emergence and patterns of the bulbar oscillation via the path $I_{odor} \rightarrow (X_o, Y_o) \rightarrow A \rightarrow (X_k, \lambda_k)$. Therefore, this model proposes that the olfactory bulb codes the odor information in the following way. First, it detects the presence of any relevant odor by the presence of a global oscillation. Second, if it detects an odor, it determines the odor identity by the specific oscillation pattern, i.e., the oscillation amplitudes and phases across the bulb, of the mode X_k that emerges. Third, the odor strengths can be roughly coded in the overall oscillation amplitudes, at least for small odor concentrations. For large odor concentrations, I_{odor} is no longer proportional to its value at a small concentration[30]. As we sometimes perceive, the character of an odor may depend on its concentration.

Absence of oscillation is apparent with absence of odor $I_{odor} = 0$, as is the case before inhalation. But some inputs may still be irrelevant or “odorless” for the animal to detect, and the bulb may choose to ignore them even when they are large. Equation (10) suggests that only those modes with non-real λ_k can emerge. Hence, only those I_{odor} that can make matrix A sufficiently asymmetric to have large non-real λ_k , will cause the bulb to respond. For illustration, consider an example when both H_o and W_o are symmetric and uniform (cyclic):

$$H_o = \begin{pmatrix} h & h' & 0 & 0\dots & 0 & h' \\ h' & h & h' & 0\dots & 0 & 0 \\ 0 & h' & h & h' & 0\dots & 0 \\ \vdots & \vdots & \ddots & & & \vdots \\ h' & 0 & \dots & 0 & h' & h \end{pmatrix} \quad W_o = \begin{pmatrix} w & 0 & 0 & 0\dots & 0 \\ 0 & w & 0 & 0\dots & 0 \\ 0 & 0 & w & 0\dots & 0 \\ \vdots & \vdots & \ddots & & \vdots \\ 0 & 0 & \dots & 0 & w \end{pmatrix}.$$

Each mitral cell only connects to the nearest granule cell with the same strength w ; each granule cell synapses on the nearest mitral cell with strength h , and, in addition, onto the mitral cells at the neighboring left and right with strength h' . If in addition, all the mitral (granule) cells are identical and receive the same receptor (central) input strength I_i ($I_{c,i}$), then by symmetry (X_o, Y_o) is uniform, i.e., each component in X_o or Y_o is the same. The matrices $G'_x(X_o)$ and $G'_y(Y_o)$ will be proportional to the identity matrix, $A = H_o G'_y(Y_o) W_o G'_x(X_o)$ is then symmetric:

$$A = \begin{pmatrix} a & b & 0 & 0 & \dots & 0 & b \\ b & a & b & 0 & \dots & 0 & 0 \\ 0 & b & a & b & 0 & \dots & 0 & 0 \\ \vdots & \vdots & & \ddots & \dots & & \vdots \\ b & 0 & \dots & 0 & b & a \end{pmatrix}$$

The N oscillation modes will be:

$$\begin{pmatrix} \sin(k1) \\ \sin(k2) \\ \vdots \\ \sin(ki) \\ \vdots \\ \sin(kN) \end{pmatrix} e^{-\alpha t \pm i\sqrt{\lambda_k} t} \quad \begin{pmatrix} \cos(k1) \\ \cos(k2) \\ \vdots \\ \cos(ki) \\ \vdots \\ \cos(kN) \end{pmatrix} e^{-\alpha t \pm i\sqrt{\lambda_k} t}$$

where $k = 2\pi\frac{K}{N}$, K is an integer, $0 \leq K < \frac{N}{2}$, $\lambda_k = a + 2b \cos(k)$. For $b < a/2$ and $\lambda_k > 0$, all the modes will be damped oscillations with similar frequencies close to \sqrt{a} . Inhalation of a “uniform odor” ($I_{odor,i} = I_{odor,j}$ for all i, j) only increases proportionally the values of a and b , and thus λ_k , but A remains symmetric and oscillations never emerge spontaneously.

The bulb can design its responsiveness to selected odors by designing its synaptic connection strengths. In the above example, the bulb ignores the “uniform odor” and only odors activating different receptors differently can possibly induce global

oscillations. However, the bulb can choose to respond to this “uniform odor” by changing the synaptic design above, e.g., by deleting the connection of each granule cell to the mitral cell to the left, i.e., $(H_o)_{i,i+1} \rightarrow 0$. Everything else staying the same, we then have a non-symmetric matrix $A \propto H_o$ with complex λ_k 's (as can be seen on a 3×3 matrix) even before inhalation, ready to be raised by the “uniform odor” to higher values to satisfy (10).

The same influence path $I_{odor} \rightarrow (X_o, Y_o) \rightarrow A \rightarrow (X_k, \lambda_k)$ makes it apparent that each I_{odor} induces a specific output to code the information by amplitude and phase pattern X_k . X_k is selected from the pool of N modes. Such a pool is itself different for different odors via a different A or dynamic system (7). Thus, there is potentially a large number of oscillation modes or a large number of odor types that can be distinguished. In our example of $N = 10$, 3 odors were observed [3]. However, it is not known how the odor number scales with system size. In principle, the frequency $Re\sqrt{\lambda}$ can also carry odor information. However, since the frequency is the same across the bulb, it only contributes to the code by one variable, negligible compared to the N variables each from the amplitudes and phases.

The bulb codes the odor strength as follows. During inhalation, the input increases at a rate proportional to the odor concentration. Hence higher odor concentrations cause $Re(-\alpha \pm i\sqrt{\lambda_k})$ to shift sooner from negative to positive values. Thus the mode X_k can grow into a higher amplitude oscillation, which can be interpreted by the olfactory cortex as a higher odor concentration. For some odors, the bulb requires a smaller concentration than for other odors to lead to an emergence of oscillation. The bulbar sensitivity can thus be higher for particular odors.

In principle, it should be possible to design the synaptic connections such that the bulb can reach a desired correspondence between odor stimuli and oscillation patterns, different sensitivities for different odors, and different resolutions to odor discrimination tasks. Here, low resolution to odor discrimination means similar oscillation pattern responses to different odor inputs. How to design the bulb connections remains an open problem.

4.2 Odor segmentation in the olfactory bulb — olfactory adaptation

It is desirable to recognize the odor components in an odor mixture instead of simply judging the mixture as a new distinctive odor, as each odor component may convey a distinct message (consider for example an odor mixture which contains odorants from two distinct sources, one a predator the other some food). Any realistic model for olfactory computation should also solve the complex problem of odor segmentation in odor mixtures. The present bulbar model does so by olfactory adaptation.

Since receptors responding to different (non-pheromonal) odors do not segregate to different groups [12], it is not possible to segment the odors by attending to different receptor groups. It was proposed [4] that, in the case of a two-odor mixture for example, this problem is solved by olfactory adaptation to one odor and recognizing the other as if it were the only odor component present. This model suggests that the olfactory adaptation should not be understood as fatigue, but as an active mechanism to screen out the current and already detected odor inputs, so that the olfactory system can concentrate on detecting new odors superposed on the existing ones. Humans have difficulty in identifying components in odor mixtures [33]. For example, two substances odorous singly may be inodorous together — counteraction; or only one odor type is sensed when two are mixed — masking [31]. Without odor adaptation, the new input odor superposed on existing ones may be masked and counteracted. Since odor receptors do not show much sign of odor adaptation [31] and the bulb on the other hand does [34], it is reasonable to believe that the odor segmentation problem is first solved in the bulb. And since adaptation is odor specific and subjects adapted to one odor can still detect new odors [31], this suggests that adaptation may involve odor specific control signals from higher olfactory centers, which have feedback paths to the bulb [1].

$$\begin{aligned} dX_o &\approx (\alpha^2 + HW)^{-1}(\alpha dI - HdI_c) \\ dY_o &\approx (\alpha^2 + WH)^{-1}(WdI + \alpha dI_c) \end{aligned} \tag{12}$$

where $I = I_{background} + I_{odor}$, $I_c = I_{c,background} + I_{c,control}$, and $I_{background}$ and $I_{c,background}$ are time invariant within a sniff cycle. The central feedback I_c is sent to the granule cells. It, like Y_o , is assumed to have dimension M (the granule cell number), while I , like X_o , has dimension N . A complete cancellation means a simultaneous satisfaction of the $N + M$ equations $dX_o = 0$ and $dY_o = 0$. This is generally impossible with only M control variables in I_c . Since mitral cells are the only bulbar output cells, one can loosen the demand and require only N equations $dX_o = 0$, which is possible in the real bulb where $M \gg N$. Then the non-oscillatory output $G_x(X_o)$ is the same as it is in the absence of odor. As a result, the oscillatory bulbar output will not exist either since its emergence requires *both* X_o and Y_o to rise above threshold to make λ large enough. We thus reach an effective means of odor adaptation.

$I_{c,control}$ is odor specific: from Eq. (12), $dX_o = 0$ leads to $dI_{c,control} = H^{-1}\alpha dI_{odor}$. It is possible for the central brain to send such an odor-specific cancelling, or adaptation, signal $I_{c,control}$, since adaptation occurs after I_{odor} has already been recognized by the brain from the previous sniff, and thus the higher olfactory centers have enough information about the odor to construct the appropriate $I_{c,control}$.

Computer simulations demonstrated successful adaptations by such a mechanism: an input odor can be fully cancelled at the bulbar output as if no odor input existed. Reducing the adaptation signal $I_{c,control}$ by half reduces the bulbar output amplitude considerably (from non-adapted situations) as if a much weaker odor were inhaled (Fig. 4). To test this model on odor segmentation, two inputs I_{odor1} and I_{odor2} representing two different odors are superposed linearly to give the odor mixture input

as $I_{odor} = I_{odor1} + I_{odor2}$. Such linear approximation for receptor inputs is assumed valid for small odor concentrations. Without any adaptation signals $I_{c,control}$, the bulbar output pattern can be seen to resemble neither output when each odor is presented alone. Then, I_{odor2} is arbitrarily chosen as the pre-existing and adapted odor, and the central feedback $I_{c,control}$ is the adapting signal specific to I_{odor2} . As demonstrated in Fig. 4, the bulb clearly responds as if only I_{odor1} were present [4], achieving odor segmentation. The success of this model depends partly on the fact that the operating region of the bulb in normal odor environment is essentially linear, as suggested by physiological experiments for small oscillation amplitudes [27], although there is a small region of non-linearity when breaking away from threshold for odor detection [4].

This adaptation model predicts that central feedback to the bulb should increase after initial exposures to an odor, and that the signal should vary on the same time scale as the breathing cycle $\sim 0.2 - 1$ second, instead of the bulbar oscillatory time scale, ~ 25 milliseconds. The feedback signal should be odor-specific and directed to the granule cells in a distributed fashion. Experimentally, not much is known of such feedback signals except that feedback paths do exist anatomically [1]. It has also been demonstrated that when the central input to the bulb is blocked, the neural oscillatory activity induced by odor stimulus increases substantially [36] — supporting our proposed source of adaptation signals. A systematic experimental study on the central feedback to the bulb will provide a crucial test of this model.

4.3 Olfactory psychophysics — cross-adaptation, sensitivity enhancement, and cross-enhancement

The bulbar model presented above also explains other olfactory psychophysics. One such phenomenon is olfactory cross-adaptation. Experiments show that after sniffing one odor, another odor at next sniff smells less strong than it normally would and may even smell different [31]. The extent to which odor A is cross-adapted by B is different from that of B by A [35]. Our model explains such cross-adaptation naturally. After exposure to odor A, the central brain sends an adapting signal that is specific to A. As recovery from olfactory adaptation takes 1-3 minutes [31] after a pre-existing odor is removed, the adapting signal will last for at least a few sniffs even after odor removal. Imagine that at the next sniff, the odor A is suddenly replaced by odor B. Since the adapting signal is specific to A, the effect of odor B on the bulb cannot be completely cancelled by the adapting signal, rather, the bulb's response to B will be distorted with the suppressive effect of the adaptation. Computer simulations confirm such a result [4].

This model can also enhance the bulb sensitivity to particular odors by reversing the adaptation signal. Sensitivity enhancement has been observed psychophysically in rats [37], but not yet in humans. Analogous to cross-adaptation is cross-enhancement,

although it is unknown whether it exists psychophysically. Both enhancement and cross-enhancement have been demonstrated in computer simulations [4].

5 A model of odor segmentation through odor fluctuation analysis

The olfactory bulb model described above applies most likely only to animals that do not depend on olfaction as the primary sense of the world. The computational tasks that model addresses are odor object detection, identification, and segmentation if multiple odors are initiated unsynchronously. Such goals are clearly not enough for animals that primarily depend on olfaction to explore their environment. These animals need olfaction to function as visual animals need vision, namely, they depend on olfaction for localizing, in addition to identifying and segmenting, odor sources with respect to their environment. A recent work by Hopfield [2] addressed this computational problem and proposed using temporal fluctuations in receptor inputs for such a purpose.

5.1 A different olfactory environment and a different task

Hopfield [2] argued that in most olfactory environments, odors are brought to the nose by fluctuating and turbulent winds, such that the odor plume contains a complex spatial structure and is increasingly mixed with odors from other parts of the environment as time increases. Thus, if there is only one odor object present, the location of its source can be obtained by analyzing the fluctuations of the odor intensity with time and relating them to the local wind directions. On the other hand, if there are multiple odor sources, each at its own location, the odor plume to the nose will contain all components with different intensities fluctuating largely independently due to complex mixings by the wind before reaching the nose. Since receptor neurons activated by different odors overlap [12], different fluctuations of multiple odors are superposed in the receptor cell responses. A separation of odors and their fluctuation signals is needed before each odor location and identity can be decoded. This is so even when the odor objects are not familiar to the animals [2]. Hopfield hypothesized that the function of the earliest part of the olfactory processing in highly olfactory animals is to achieve this separation task, such that the contributions of different odor sources to the receptor activities can be separated.

Both this model and the previous one presented in last section address the odor segmentation task. However, there are major differences between the two. First, the olfactory environments are different. In Hopfield's model, the odor intensity fluctuates on a time scale of tens of milliseconds [38]. The previous model assumes

an environment that changes slowly, on a time scale longer than the breathing cycle, before reaching the olfactory mucosa where the breathing modulates its effects on the receptors. Second, the segmentation tasks are different. The slowly changing environment allows the previous model to segment mixed odors by subtracting out the pre-existing odors, but it cannot do so when each odor component in the mixture is initiated at the same time. Hopfield’s model does not simply subtract out one odor in the mixture, as the fast fluctuations make it difficult. Rather, it *simultaneously* sorts out individual odor fluctuations from the mixed multisource input signals.

Behavioral evidence [39] demonstrates that olfactory animals such as the terrestrial mollusc *Limax maximus* [40] use the time fluctuations for olfactory tasks. When two odors are completely mixed and originate from the same spatial location, and thus have the same temporal fluctuations in their intensities, they are recognized as one distinct odor different from the two component odors. But as long as there are differences in temporal fluctuations in the two components — for example, placing the odor sources at even slightly different locations — the two odors are individually identified [40]. We will describe below how Hopfield’s model achieves similar performances in cases of independent odor component fluctuations.

5.2 Odor segmentation in an adaptive network

An idealization of olfactory bulb circuitry was used [2]. However, the odor information coding is qualitatively different from the previous model. First, the synaptic strengths between the cells adapt to the odor inputs, an essential feature for the functioning of Hopfield’s model. Second, the odor identity information is coded by the synaptic strengths rather than by the cell activities, which instead code the instantaneous odor strengths.

A network of linear and mutually inhibitory neurons is used [2], each neuron is denoted as x_i in the state vector of $X = \{x_1, x_2, \dots, x_N\}$. The cell dynamics are (to compare with the previous model, the notations are modified from that of [2]):

$$\dot{X} = -TX - \alpha X + I \tag{13}$$

This can be seen as a drastic simplification from (1), by assuming $G_x(x) = x$ and $G_y(y) = y$, ignoring central inputs I_c , and assuming that the granule cells instantaneously follow their inputs from mitral cells such that $Y \propto W_o X$. Substituting Y into equation (6) and assuming $T \propto H_o W_o$, we obtain Eq. (13) where the mitral cells effectively inhibit each other.

The odor input I differs from the previous model in its temporal courses to reflect the odor concentration fluctuations instead of the regular respiration. Each odor k

at some unit concentration is assumed to excite the mitral cell i with strength S_{ki} . Its concentration is described by a fluctuating time function $a_k(t)$. Thus, the input to the i^{th} mitral cell will also fluctuate with t as

$$I_i(t) = \sum_k a_k(t) S_{ki} \quad (14)$$

Let us now look closer at the segmentation problem. There are two modules of the segmentation needed. The first is to segment the *odor concentrations* $a_k(t)$, and second is the *odor identity* defined by S_{ki} , for all odors k . Both of these signals are mixed in the inputs I . Because each odor excites many mitral cells, independent odor fluctuations $a_k(t)$ for different odors k will result in *correlated* fluctuations in inputs $I_i(t)$ to different cells i . It is these *correlations* that define the individual odor objects for the olfactory system [2]. This crucially requires that individual odor fluctuations themselves are uncorrelated, otherwise “olfactory illusions” should occur [2]. The idea is then to transform the correlated receptor inputs I to mitral outputs X such that first, the components of X , unlike I , are *uncorrelated*; second, X still carries all the temporal information in I . This is possible if each component x_i depends on no more than one odor component concentration a_k , which in turn is carried in the activity of only one output cell. This way, the first module of odor segmentation — to segment the individual odor concentration a_k from I — is achieved at the X level, and the higher olfactory centers only need to look at one component of X for each a_k .

Let us see if such decorrelation (segmentation of a_k) also leads to the segmentation of S_{ki} , the second module of the segmentation task. To achieve this decorrelation at X , the synaptic connections T should satisfy some conditions depending on the odor, or in other words, T should have the knowledge of the individual odor components S_{ki} . It would be ideal if, in the case that mitral cell n (x_n) carries concentration fluctuation of odor k , the odor identity information S_{ki} is carried in synapses T_{ni} or T_{in} associated with the *same* cell n . This would not only segment the odor identity S_{ki} , but also tag this piece of information to the same cell that carries this odor’s concentration. Using an example of a two-odor mixture [2], and the simplification of small $\tau \equiv 1/\alpha$ such that one can assume $\dot{x}_i \approx 0$ for all t , we see that such segmentations are possible [2]: If, e.g., the first column of matrix $\alpha + T$ is the vector S_1 and the second column S_2 , then $x_1 = a_1$, $x_2 = a_2$, and $x_{i>2} = 0$. Thus all cells are inactive except for two output cells which convey the odor strengths for the respective odors, and their synaptic strengths to other cells, i.e., T_{i1} and T_{i2} respectively, carry the odor identities S_{1i} and S_{2i} respectively.

It is now clear that such tasks require T to adaptively change as the odor sources change with the environment. Hopfield [2] proposed the following synaptic dynamics in addition to the cell dynamics above:

$$\dot{T}_{ij} = f x_i \cdot f x_j [\delta + \epsilon (f x_j - \gamma f x_i)] \quad (15)$$

where fx_i is a high-pass filtered version of x_i , δ , ϵ , and γ are constants determining the learning speed, which should be much slower than the cell dynamic speed. Such a synaptic changing rule is local and depends only on the pre- and postsynaptic neurons. The synapses T will stop changing when each cell n is assigned to a different odor k , $x_n = a_k$, or inactive, $x_n = 0$. In that case, all the terms on the right side of (15) vanish under time average when odor fluctuations are independent. Thus equations (13) and (15) give the desired performance. Furthermore, the desired solution for T is stable in the sense that if T is close to the solution, convergence is guaranteed [2].

This adaptive network demonstrates its performance in a computer simulation [2], with six neurons and a two-odor mixture. Fig. 5 shows that before synaptic learning, all six neurons fluctuate with the inputs, while after synaptic learning is turned on only neurons 3 and 6 keep their responses to follow odors B and A respectively. These two neurons happen to be the recipients of the strongest components S_{ki} for the respective odors (i.e., $(k, i) = (B, 3)$ and $(A, 6)$), since the inhibition between neurons resulted in the winner-take-all type output configurations. The final synaptic strengths T_{i3} and T_{i6} from neurons 3 and 6 code the odor identities S_{B_i} and S_{A_i} for odors B and A respectively. Such a network should also forget its synaptic strengths with vanished cell activity, so that it can adapt to new odor mixtures with new inputs from the environment. Here, the synaptic adaptation captures odor quality information S . One should notice that adaptation in this model does not mean to lose the perception to the odors as in the previous model.

The higher olfactory centers have to somehow query the synaptic strength T to get the information about the odor identity S_{ki} . They need to send a signal to the dendrites of the principle neuron that is reporting the concentration of the odor, and reads out the responses of the other neurons to that signal. Hopfield suggests one possible way to do this by multiplexing these signals on the same neuronal axons reporting the odor strengths. The low frequency component of the signals carries the odor concentration signal while the higher frequency component signals carry the odor identity S_{ki} information [2]. Another possible mechanism was suggested in [41]. One can have multiple copies of the network receiving the same odor inputs, each neuron in m^{th} network inhibits its copies in all n^{th} ($n > m$) networks such that at the end of adaptation (equation 15), each network has a different neuron reporting the corresponding odor fluctuation. Since the adaptation selects the winner neuron for each odor, extending the example of two odors above, the first network selects the two neurons, 3 and 6, most activated by the two odors respectively; the second network selects the two second most activated, e.g., 4 and 5, respectively, etc. The covariation between the neurons in different networks assigns them to the same odor. The odor concentration can be read out from the corresponding neuron in any network, while the identities of these neurons code the odor quality S_{ik} . A modification to make different networks receive different, maybe overlapping, subsets of receptor inputs, simulating glomeruli structure, could make the model more biologically plausible [41]. This mechanism makes it possible to have interesting psychophysics phenomena similar to cross-adaptation. If new odors are introduced before synaptic recovery

from the previous odors, the winner neurons for the previous odors are more likely to remain winners by the advantage of their already developed inhibitory synapses over others. Thus the winning neurons might be different from those if the new odors were introduced without prior odor exposures, resulting in distorted odor identity information. Preliminary simulations in a six neuron network exposed to two odors [42] confirmed such a possibility, although it does not happen most of the time.

The present model segments the odor sources even before the odor qualities are known [2]. This demonstrates the model capability to capture the invariants in the varying sensory inputs. In a typical olfactory environment, although the receptor inputs I fluctuate with time, the odor qualities S_{ki} are constant at least for a short period of time, and there should be a perceptual constancy. In most cases, the number of neurons N is larger than the number of odors K . The variation of the input I in the N dimensional input space, ignoring noises, should be confined to a K dimensional subspace, reflecting the regularities in the inputs carrying the constant odor qualities. This means, the matrix R defined by input covariance

$$R_{ij} \equiv \langle (I_i - \langle I_i \rangle)(I_j - \langle I_j \rangle) \rangle = \sum_k (a_k - \langle a_k \rangle)^2 S_{ki} S_{kj}$$

has only K eigenvalues that are substantially non-zero. This input regularity enables the network to find the K dimensional subspace, spanned by the K eigenvectors corresponding to the first K non-zero eigenvalues of R (i.e., to find the K principle components of the input variations). Furthermore, the network identifies the K axes or directions S_{ki} for $k = 1, 2, \dots, K$, not necessarily orthogonal to each other, in that subspace representing the odor qualities. As we know, except when there is only one odor $K = 1$, there are infinitely many choices of axes or directions to span a $K > 1$ dimensional space. S_{ki} in most cases are not in the directions of the individual eigenvectors (principle components). Not being able to identify them would result in confused odor quality perceptions. However, the non-Gaussian property of the fluctuating concentration $a_k(t)$, e.g., the non-zero third moments $\langle a_k^3 \rangle$ about the mean, is another regularity of the inputs that enables the network to decipher the odor quality [2]. Such positive third moments are assumed [2] as the odor strength distribution is expected to have longer tails above the mean.

The network, including the learning rule, has no prior knowledge of the odor quality, other than the non-Gaussian statistical knowledge of the odor fluctuation a_k . The ϵ term of the learning rule (15) takes advantage of this non-Gaussian property to capture the odor quality S_{ki} . The learning stops when both the covariance $\langle f x_i f x_j \rangle$ and the correlation $\langle (f x_i)^2 f x_j \rangle$ between neurons vanish. Since the third moment $a_k^3 \neq 0$, the elimination of third order correlation $\langle (f x_i)^2 f x_j \rangle = 0$, by the ϵ term, is essential to ensure that the activity of each output neuron depends on no more than one odor fluctuation.

The present model thus gives an entirely different way of thinking about the synaptic connections [2]. Unlike conventional neural networks, the synapses code the sensory

information, and are more than just algorithms to compute. There are no matched filters for the odors in the connections until after the successful adaptation. In a sense, recognition can be understood as the capability of adaptation. This is also reflected in the previous model where adaptation, although of a different nature, was possible only when the higher olfactory centers have the odor information. Fast synaptic modulation has been advocated by others as a computational element [43]. It has also been recently used in another olfactory model where the inhibitory synapses adjust to transform redundant responses in the receptor population to a more efficient representation at the output neurons [16].

6 Discussion

Two models of the early olfactory computation have been presented. One [3][4] samples the environment by discrete breathing cycles; during each cycle the environment is assumed to change little. It codes the receptor inputs into a coherent oscillatory output pattern, to be identified as a single distinct odor. It does not follow the fluctuations of the odor strength on a time scale shorter than the breathing cycle, and thus cannot as easily decode the odor source locations by the fluctuation analysis. It segments two coexisting odors when one of them is present before the other appears, by subtracting the earlier odor background and thus recognizing the later one. The other model [2] samples the environment continuously, following the details of the input fluctuations which have a shorter time scale than the odor recognition process. It segments odor mixtures without the need to subtract out individual odors and can thus achieve simultaneous recognition. The neural output carries the time fluctuations of the odors which may be used to compute source locations, while the odor identities have to be determined from the synaptic strengths of the output neurons.

The two models differ dramatically in their tasks and computational mechanisms. Leaving aside the difference in mechanisms, it is not certain if different tasks are emphasized in different animals or in different environmental conditions. Highly olfactory animals certainly need to emphasize more on the odor source localization task than visual animals, which may also rely heavily on olfaction when visual function alone is not enough, e.g., when hunting at night or searching for plant seeds under heavy leaves [44]. Insects seem to have a much higher sensitivity to odors than humans do [31]. This enables them to detect small odor intensity variations which occur on a very short time scale, around 10-100 milliseconds in the outdoor environment [38]. This is possible also because their receptor cells have a time constant around 10 milliseconds [6]. The lower animals also have their olfactory reception decoupled from their respiratory mechanism, enabling them to follow the odor fluctuations undisturbed and undisrupted. The vertebrate receptor neurons, on the other hand, have a long time constant, about 200 milliseconds [12], comparable to the breathing time scale in mammals (e.g., rats [44], although we humans breath once every 4 seconds). Such a long time constant makes it difficult to detect odor fluctuations on a

finer time scale, and may be a necessary strategy for an insensitive receptor neuron to integrate the signal in time to increase the signal-to-noise ratio. However, since there is also a long time scale fluctuation in odor concentration of natural environment [38] — periods of about a couple hundred milliseconds of relatively strong odor concentration separated by periods of weak odor concentration — it is conceivable that this longer time scale variation can also be used for odor orientation. In an indoor environment, like the underground burrows of rodents, air is much less turbulent and air flow speed is an order of 10 times slower than it is outdoor. (You can test this by blowing soap bubbles and watching them flow in the air.) The odor fluctuation will be much slower, as we notice in the kitchen of an apartment, for example. Such an environment will have a long lasting background odor, and an odor adaptation model [4] to subtract the background is conceivably used for odor segmentation.

However, behavioral evidences clearly point to olfactory cues used even in many mammals for object localization. For example, sunflower seeds and hazel nuts under the soil surface can be localized by mice; large cats can be observed to sniff the wind continually and usually approach their preys from downwind [44]. It is conceivable that many mammals also use temporal fluctuations of odors, although maybe on a longer time scale, to locate odor sources. Another possible odor localization mechanism maybe to compare the odor concentrations between the two nostrils, tentacles, or antennas. Observations from humans [45] to honeybees [39] indicate that a 10% difference in odor concentrations between the two sides is enough to make bilateral behavioral judgement on the odor source direction. It was shown that damaging one tentacle or antenna induces the experimental animals to turn towards the undamaged side in search of the odor source [46][39], supporting the stereo-olfactory mechanism. Many animals, e.g., hammerhead sharks, have their two nares widely separated [44] presumably for the purpose of odor source localization. The two olfactory bulbs, each receiving inputs from the corresponding epithelium, interact with each other by connections from the mitral cells to the contralateral granule cells via anterior olfactory nucleus [47]. Therefore, the two olfactory bulbs may be the first stage where the stereo-information gets processed.

On the other hand, it has also been observed that some animals can still localize odors after one tentacle is damaged [46], or after the animal overcomes the initial confusion caused by the damaged tentacle [39]. Temporal analysis of odor concentrations is presumable used and sufficient in many cases. It is conceivable that temporal fluctuation analysis and stereo-olfaction are used in parallel or complementarily in many animals. Imagine a situation, for instance, when there are two spatially separated sources with identical odor substance (e.g., two pheromone emitting females for a male animal), they would be seen by present early olfaction model as one single odor source whose time fluctuation is a superposition of the fluctuations from the two sources. The higher olfactory centers need to decouple the fluctuating sequence into two separate ones, maybe by filtering the signal with two different temporal filters. This requires additional knowledge of the environment [2], e.g., maybe by using wind sensor signals and/or assuming different temporal characteristic time constants

for the two component fluctuations. This problem is just as difficult, if not more, if stereo-olfaction mechanism alone were used to localize the two sources. However, combining the temporal analysis and stereo-olfaction mechanisms would certainly give an edge, by maybe analyzing the correlations between the signals in the two nares — if there were only one source, the correlation would be different. Some animals swing their heads from side to side, or take a zig-zag path towards a odor source, sampling odor concentration at different spatial *and* temporal locations [39]. Such maneuver suggests the use of a combination of spatial and temporal analysis, and would be more important for animals of smaller body sizes.

The first bulb model [3][4], subject to interruption by exhalation, will change its oscillation patterns and amplitudes as the odor mixture inputs fluctuate. It is not clear how it can simultaneously segment component identities and fluctuations in the mixed input fluctuating with a short characteristic time. In a typical outdoor environment, odor concentrations fluctuate with pulses of strong intensities lasting about several hundred millisecond, separated by inter-pulses of low odor intensities lasting about 5 times longer [38]. In the case of low sensitivity and long time constants of the receptor neurons, the bulb may perceives one odor at each sniff in an environment of two dominant odor mixtures fluctuating independently, the other odor during its inter-pulse and the distant faint odors would be unnoticed. In this case, the component segmentation is approximately achieved by separate sniffs, the bulb could then in principle follow each odor fluctuation on the time scale of the sniff cycle. To incorporate stereo-olfaction, interbulb interaction should be introduced into the bulb.

Hopfield's model[2] should be sufficient for most olfactory environments even without stereo-olfaction, provided that the higher olfactory centers could disentangle the superposed concentration fluctuations. (This is analogous to individuals of only one functional eye, they segment the visual objects by imposing other constraints of the visual environment, e.g., motion and shape from shading [2].) Since the biologically realistic bulbs oscillate, it remains to be seen whether the temporal fluctuation analysis model performs well when both the excitatory and inhibitory cell interactions are included.

Instead of using a static neural activity pattern, our first model uses oscillatory patterns to code odor information, starting from an odor input that is comparatively much less oscillatory. The olfactory cortex, which receives inputs from the olfactory bulb, is also intrinsically oscillatory. An intriguing possible explanation for the oscillatory nature of the cortex is that the oscillations may provide a natural mechanism for decoding its inputs, for example by selectively resonating with inputs of specific amplitude and phase patterns as well as frequency. The second model codes the odor identity by synaptic strengths instead of neural activities, extending the role of synaptic strengths from merely algorithms of computation to information carriers. Recently, a model of the specialist olfactory system of insects [15] suggested coding by response duration, latency, and other variations in the temporal response

for the input mixture ratios, input temporal profiles, and frequency, etc. which are behaviorally relevant. Coding by synaptic strengths, oscillation patterns [48], complex neural temporal structures [49], and using signal correlations for object binding or recognition could be used in many other computational contexts [2]. Interacting groups of excitatory and inhibitory neurons are ubiquitous in other cortical areas [1] and can be easily modelled by extending equation (1) [3].

The computational approaches used in the models are likely to apply to more than the olfaction. Adaptation to pre-existing stimuli also happens in vision right at the first stage — the retina. The blood vessels in our eyes form a permanent and stationary image on our retina, we ourselves usually do not see them (although we can if we quickly flash a bright light very near our eyes) since our eyes have adapted to them in order not to be distracted to see other visual inputs. Adaptation in this sense can be seen as a mechanism to eliminate the temporal redundancy in the input information, so that output information is dominated by more recent sensory events. In Hopfield’s model, adaptation is a mechanism to eliminate spatial redundancies (correlation) in the sensory input, by constructing matched filters for odors in the synaptic connections, resulting in uncorrelated outputs. In vision, for instance, the retinal output ganglion cells have center-surround receptive fields structure to respond to input spatial contrast [50] instead of input luminance, since input luminance at nearby receptors are correlated. Hence the ganglion cells have much less correlated activities than the photoreceptors. The matched filters or receptive fields indicate the knowledge acquired by the sensory system about the environment [51][52]. In Hopfield’s model, the knowledge is the odor identity at that moment, in the retina it is the power spectrum of the input image ensemble [52].

Similarly, the olfactory perceptual shifts, such as cross-adaptation, have their analogy in vision as illusions and perceptual changes in special situations. One example is the “waterfall effect” [53]: after staring for a long time at a waterfall, stationary objects appear to move upwards. Another example is color hue shifts in perception after human subjects are exposed to an unnatural chromatic environment [54]. Theoretically, it has been proposed that the sensory after-effects are the results of efficient coding schemes for a new environment [53][55], and quantitative predictions of the post-adaptation color hue shifts have been compared with the measurements in psychophysical experiments with reasonable agreements [56]. We hope that similar progresses in olfactory areas will occur when more systematic quantification of odor molecules and receptor codings become available. In both olfaction and vision, adaptation should not be thought of as fatigue, but a computational mechanism to reduce the spatio-temporal redundancy inherent in the input signals [51][52].

Perceptual constancy, such as the odor quality (S_{ki}) captured by the synapses T in Hopfield’s model, enables the observer to recognize objects and remain oriented in the environment despite changes in the physical stimulus. The odor source location, conveyed by the temporal profile of the concentration changes, should also be perceptually invariant irrespective of the concentration scale. A recent olfactory model

of insects [15] observed such model neuronal responses depending only on the input profiles. There are also observations that perceived odor intensity stays the same for gentle and strong sniffs, but changes with the flow rate of odorized air, generated by olfactometers, in the nasal cavity [57], suggesting subjective compensations for the observation mode to achieve odor concentration constancy. Analogous constancies occur in vision and audition. For instance, color perception (spectral reflectance) of objects stays the same irrespective of the illuminance spectrum [58] (color constancy), recognition of visual objects should not depend on the locations and distances from the observer [59], and speech can be understood independent of the pitches of the speakers.

In summary, two olfactory bulb models have been presented as examples to discuss the computational tasks, environments, and mechanisms in olfaction. Studying olfaction can hopefully give us insights on the principles of computation in other sensory modalities.

7 Acknowledgement

I wish to thank J. Atick, S. Frautschi, A. Herz, J. Hopfield, M. Lyons, and M. Newton for carefully reading the draft and manuscript of this paper, and for very helpful comments, especially by J. Hopfield and M. Lyons.

References

- [1] G. M. Shepherd *The synaptic organization of the brain*. Second Ed. 1979, Third Ed. 1990.
- [2] J. J. Hopfield *Proc. Natl. Acad. Sci. USA* **88** 6462-6466, 1991.
- [3] . Li J.J. Hopfield *Biol. Cybern.* **61** 379-392 (1989).
- [4] Z. Li *Biol. Cybern.* **62** 349-361 (1990).
- [5] R. H. Wright *The Science of Smell*, Basic Books Inc. New York 1964.
- [6] K. E. Kaissling *Handbook of Sensory Physiology IV Chemical Senses Part I* L. M. Beidler Ed. p 351 - 431.

- [7] W.J. Freeman *Electroencephalogr. Clin. Neurophysiol.* **44**586-605 (1978).
- [8] W. J. Freeman and K. A. Grajski *Behav. Neurosci.* 101, p766-777 1987
- [9] G.M. Shepherd *Microsc. Res.* **24**(2) p.106 (1993).
- [10] E. D. Adrian *Br. Med. Bull* 6: p.330-333 (1950)
- [11] J. L. Davis, H. Eichenbaum Olfaction — A model system for computational neuroscience, MIT Press (1990).
- [12] G. M. Shepherd In *Olfaction — A model system for computational neuroscience* Ed. J.L. Davis H. Eichenbaum H. p 225-250. MIT Press (1990).
- [13] M. Wilson, J.M. Bower In C. Koch and I. Segev (Eds.), *Methods in neuronal modeling: From synapses to networks* p 291-334. Cambridge Mass: MIT Press.
- [14] H. Liljenstrom *Int. J. Neural Sys.* 2, 1-15 (1991).
- [15] C. Linster C. Masson M. Kerszberg, L. Personnaz, G. Dreyfus *Neural Computation* **5** p 228-241 (1993).
- [16] J-C. Fort and J-P Rospars *C. R. Acad. Sci. Paris* t. 315, Serie III p. 331-336 1992.
- [17] G. Lynch, R. Granger In *Olfaction — A model system for computational neuroscience* Ed. J.L. Davis and H. Eichenbaum p. 141-166. MIT Press (1990).
- [18] M.E. Hasselmo *Neural Comp* **5** p. 32-44 (1993).
- [19] E Fransen, A Lansner, and Hl Liljenstrom in "Computation and Neural Systems 1992", Kluwer Academic Publ. (In press) 1992.
- [20] W.J. Freeman, C.A. Skarda *Brain Res. Rev***10** 147-175 (1985)
- [21] T.V. Getchell, G.M. Shepherd *J. Physiol.* **282** 521-540. (1978)
- [22] L. Buck, R. Axel: *Cell* **65** (1) 175-187 (1991)
- [23] D. Lancet, C.A. Greet, J. S. Kauer, G.M. Shepherd *Proc. Natl. Acad. Sci. USA* **79**670-674 (1982).
- [24] W.J. Freeman, W.S. Schneider *Psychophysiology***19**44-56 (1982).
- [25] E.C. Sobel, D. W. Tank. Preprint, AT&T Bell Laboratory.
- [26] A. Gelperin, D. W. Tank *Nature* Vol. 345, p. 437-440, 1990.
- [27] W. J. Freeman *Biol. Cybernetics***33**, 237-247 (1979).
- [28] K. R. Delaney, A. Gelperin, M. S. Fee, J. A. Flores, R. Gervais, D. W. Tank, D. Kleinfeld, Submitted for publication 1993.

- [29] G.M. Shepherd Private communications 1988.
- [30] B. Johnson, R. Viogt, C. Merrill, J. Atema *Brain Research Bulletin* **26**(3):327-331 (1991)
- [31] R.W. Moncrieff R. W. The chemical senses, CRC Press Third Ed. (1967)
- [32] F.H. Eeckman Statistical Correlations between Unit-Firing and Cortical EEG. Thesis, University of California, Berkeley, 1988.
- [33] D.G. Laing, A. Glemarec *Physiol. & Behavior* **52** (6) p.1047-1053 (1992)
- [34] M. A. Chaput, H. Panhuber *Brain Research* **250**41-52 1982
- [35] W.S. Cain T. Engen, In *Olfaction and taste*, C. Pfaffmann (Ed.) New York, Rockefeller Press, p. 127-141 (1969).
- [36] C.M. Gray, J.E. Skinner *Exp Brain Res.***69**378-386 (1988)
- [37] D. G. Laing A. Mackay-Sim In D. A. Denton and J. P Coghlan (Eds.), *Olfaction and taste*, V. New York: Academic Perss, 1975. p. 291-295.
- [38] J. Murlis, C.C.Jones *Physiological Entomology* **6**71-86 (1981)
- [39] W. J. Bell and T. R. Tobin *Biol. Rev.* **57** 219-260 1982.
- [40] J.F. Hopfield, A. Gelperin *Bahav. Neurosci.* **103** 329-333 (1989)
- [41] O. Hendin, D. Horn, J.J. Hopfield. Preprint (1993); D. Horn Private communications (1993).
- [42] Simulations done by O. Hendin and myself (1993).
- [43] C. von der Malsburg, E. Bienenstock In *Disordered Systems and Biological Organization* eds. E. Bienenstock, E., Fogelman Soulie, F. Weisbuch G. Springer, Berlin 247-252 (1985). Oxford University Press 1979
- [44] D. M. Stoddart *The Ecology of Vertebrate Olfaction*, Chapman and Hall, 1980.
- [45] G. von Bekesy *J. appl. Physiol.* **19**, 369-73 (1964)
- [46] R.P. Croll *Biol. Rev.* **58** p.293-319 (1983)
- [47] Schoenfeld, Macrides *J. Comp. Neurol.* 227:121 (1984).
- [48] C. Gray, W. Singer *Nature (London)* **338** 334-337 (1989)
- [49] J. W. McClurkin, L.M. Optican, B, J. Richmond, and T. J. Gawne *Science* **453** p. 675-677 (1991).
- [50] E. R. Kandel and J. H. Schwartz *Principles of Neural Science*, 2nd edition, Elsevier (1984).

- [51] H. B. Barlow (1961) p. 217-234 In *Sensory Communication* W. A. Rosenblith, ed. MIT Press Cambridge, MA. and p. 331-360 in *Current Problems in naimal behavior* W.H. Thorpe and O.L. Zangwill Cambridge (1961).
- [52] J.J. Atick *Network* **3** 213-251 (1992)
- [53] H. B. Barlow *Vision: coding and efficiency* p. 363-375. C. Blakemore (Ed). Cambridge university Press 1990.
- [54] M.A. Webster and J. D. Mollon *Nature* 349, p235-238
- [55] H. B. Barlow and P. Foldiak In *The computing neuron* New York: Addison-Wesley. (1989)
- [56] J.J. Atick, Z. Li, A.N. Redlich *Vision Res.* **33**(1) 123-129 (1993)
- [57] T. Engen *The perception of odors* Academic press 1982.
- [58] E.H. Land *Sci. Am.* **237** 108-129 (1977)
- [59] Z. Li and J.J. Atick *Neural Computation*, in press.

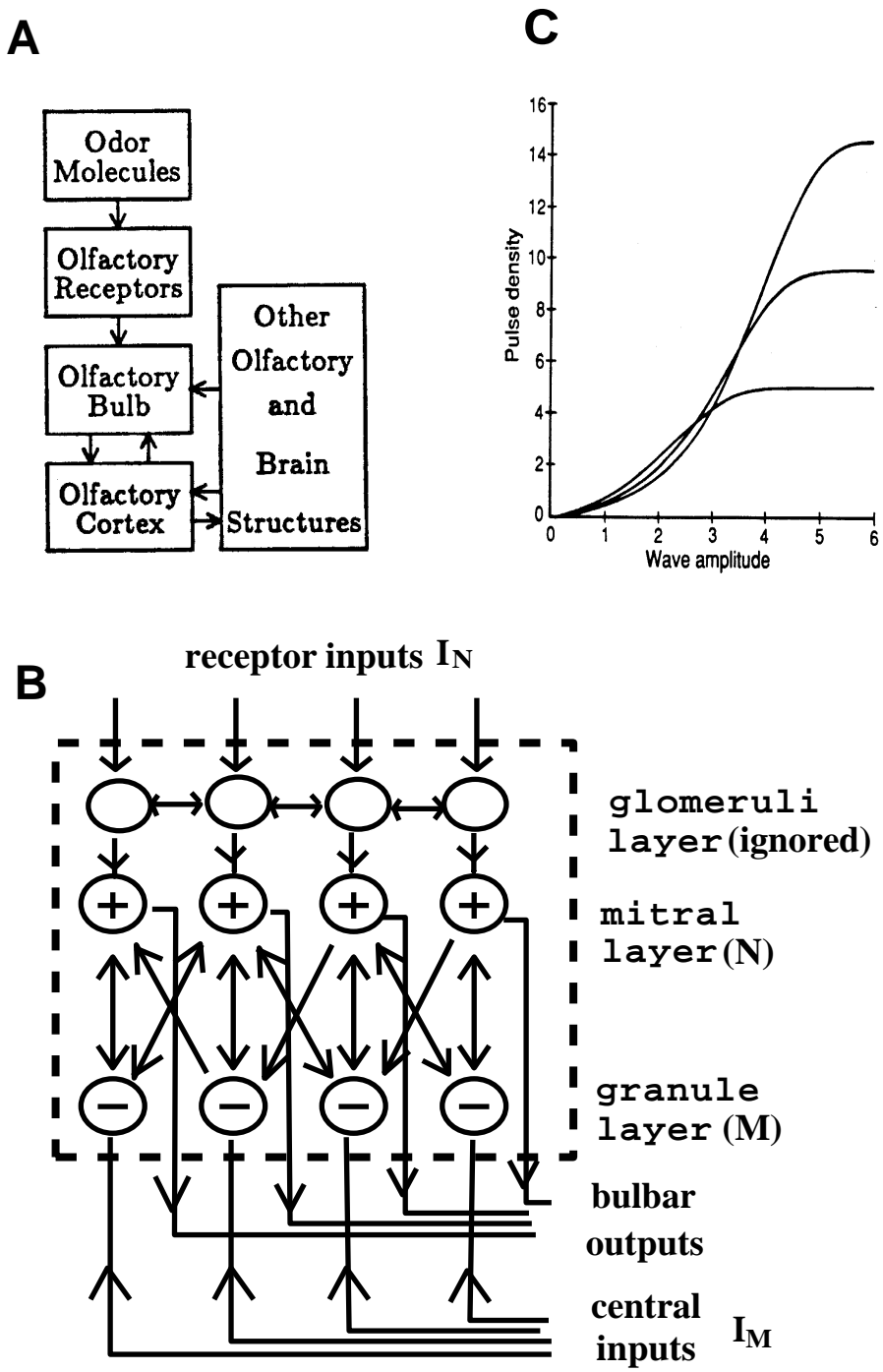


Figure 1: **A**: Olfactory system block diagram. **B**: Olfactory bulb structure, circles with '+' signs are excitatory mitral cells; with '-' signs are inhibitory granule cells. **C**: Three examples of experimentally measured functions (taken from [20]), relating the pulse probability of single or small groups of mitral cells to the EEG wave amplitudes. This function is used to model the cell input output relationships[20].

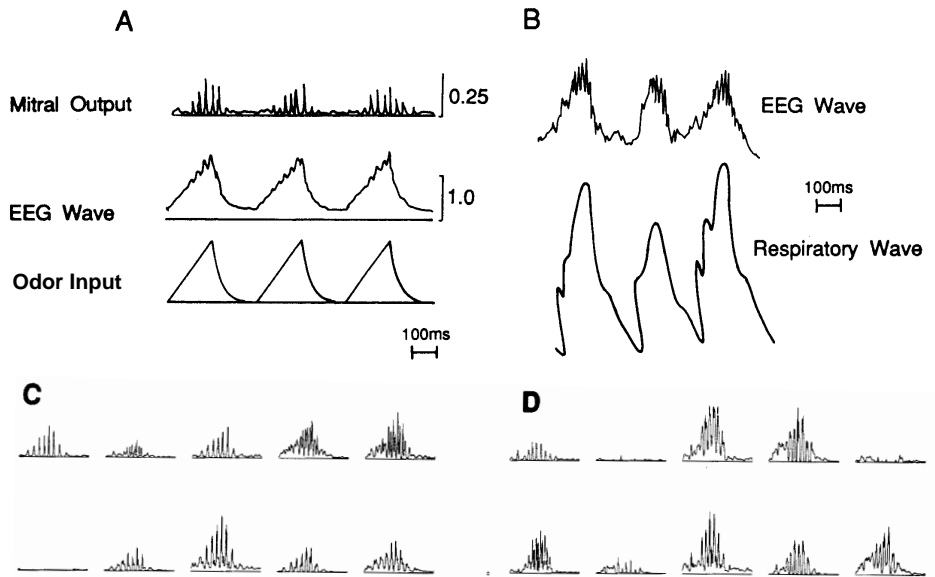


Figure 2
 Figure 2: **A:** Simulation results of output from one mitral cell and EEG waves during three breathing cycles of odor inputs. **B:** experimentally measured EEG waves with odor inputs, taken from [24]. **C:** outputs from the 10 mitral cells during one breathing cycle for a particular odor input I_{odor} . Each cell oscillates with a particular amplitude and phase, depending on I_{odor} . **D:** same as **C**, but with a different I_{odor} .

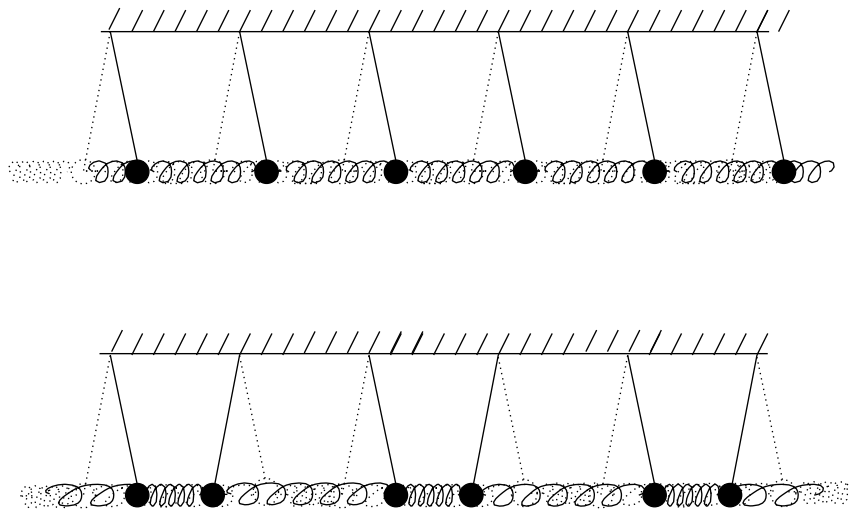


Figure 3: Two example modes in a system of coupled pendulums. The upper one has all the pendulums oscillating with the same amplitude and phase, back and forth from right (solid positions) to left (dashed positions). Each pendulum in the mode of the bottom figure oscillates 180° out of phase from its neighbors.

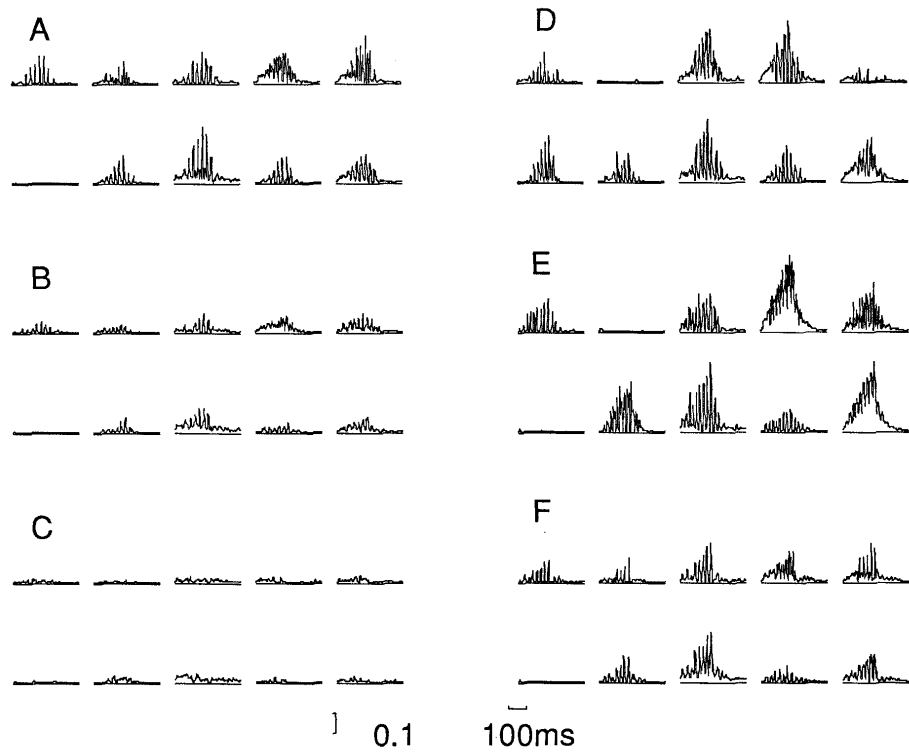


Figure 4

Figure 4: **A, B, C**: Model response to I_{odor1} without adaptation, with half strength adaptation, and with full strength adaptation to I_{odor1} , respectively. **D**: model response to I_{odor2} . **E**: model response to odor mixture of I_{odor1} and I_{odor2} . **F**: model response to the same odor mixture with adaptation to I_{odor2} — odor segmentation and detection of I_{odor1} in the mixture.

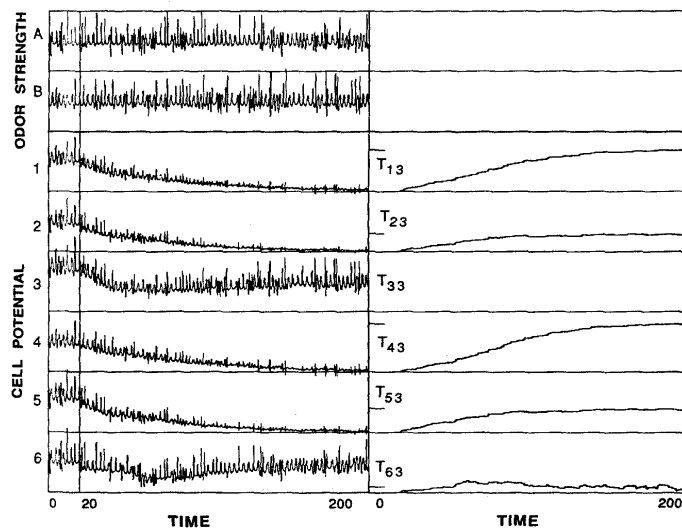


Figure 5

Figure 5: Simulation for a bulb of 6 neurons and two independent sources A and B. Synapse change begins at $t = 20$. On the left are odor strengths fluctuations and cell potential variations with time. On the right are synaptic strength development T_{n3} from neuron 3 to other neurons. These strengths carry the odor identity information S_{Bi} for odor B whose time variation is captured by neuron 3. Taken from Hopfield 1991 [2].